Journal of Inflammation Research

Dovepress
Taylor & Francis Group

Open Access Full Text Article

ORIGINAL RESEARCH

Potential Metabolic Markers in the Tongue Coating of Chronic Gastritis Patients for Distinguishing Between Cold Dampness Pattern and Damp Heat Pattern in Traditional Chinese Medicine Diagnosis

Shaojie Yuan[1], Renling Zhang[2], Zhujing Zhu[2], Xuan Zhou[1], Hairun Zhang[1], Xinwei Li[1], Yiming Hao[1]

[1]Shanghai Key Laboratory of Health Identification and Assessment/Laboratory of TCM Four Diagnostic Information, Shanghai University of Traditional Chinese Medicine, Shanghai, 201203, People's Republic of China; [2]Longhua Hospital Affiliated to Shanghai University of Traditional Chinese Medicine, Shanghai, 200032, People's Republic of China

Correspondence: Yiming Hao, Email hymjj888@163.com

Background: Dampness pattern, a prevalent traditional Chinese medicine (TCM) pattern in chronic gastritis (CG), includes cold dampness (CD) and damp heat (DH) patterns. Tongue coating differences are key diagnostic markers, yet molecular-level analyses are lacking. We applied metabolomics to identify differential metabolites distinguishing these patterns.

Methods: In this study, the first principal component was analyzed by the OPLS-DA model. The model quality was evaluated by 7-fold cross-validation, and the model validity was evaluated based on R^2Y (interpretability of categorical variable Y) and Q^2 (predictability of the model), and the permutation test was used for further verification. Strict criteria were used for differential metabolite screening. The Euclidean distance matrix of the quantitative values of differential metabolites was calculated, and cluster analysis was performed using the complete linkage method. All pathways mapped by human differential metabolites were retrieved through the KEGG (Kyoto Encyclopedia of Genes and Genomes) Pathway database, and key pathways were screened out by combining enrichment and topological analysis. The spearman algorithm was used to calculate the correlation coefficient and P value matrix. Finally, the effect of the binary classifier was evaluated by drawing the receiver operating characteristic curve (ROC curve) and calculating the area under the curve (AUC), and the combination with the highest AUC was selected as the optimal diagnostic model.

Results: Twenty significant differential metabolites emerged ($P<0.05$). Pathway analysis highlighted three key pathways, notably glycerophospholipid metabolism involving phosphatidylethanolamine. Phenol-based models showed optimal diagnostic performance (highest AUC).

Conclusion: Metabolite profiles significantly differed between CD and DH. Glycerophospholipid metabolism was central, with phosphatidylethanolamine as a key metabolite. Phenol requires further validation as a diagnostic biomarker. These findings advance quantitative diagnosis and mechanistic insights into TCM dampness syndrome in CG.

Keywords: metabolomics, tongue coating, chronic gastritis, GC-TOF-MS and UHPLC-QE-MS, diagnostic biomarker

Introduction

Chronic gastritis (CG) is a chronic inflammatory disease characterised by the infiltration of the gastric mucosa by inflammatory cells.[1] CG is a prevalent condition in China. In clinical settings, CG is manifested by a constellation of symptoms, including abdominal discomfort, nausea, vomiting, loss of appetite, and weight loss.[2] Long-term use of non-steroidal anti-inflammatory drugs (NSAIDs), helicobacter pylori infection, and bile reflux are common factors in CG,[3,4] A study has demonstrated that gastric cancer is closely associated with long-term chronic inflammation of the gastric mucosa.[5] Consequently, the early diagnosis and intervention of CG is of great significance in the slowing down of the progression of chronic gastritis and the prevention of gastric

Received: 26 July 2024
Accepted: 9 July 2025
Published: 23 July 2025

cancer. Currently, the only biochemical markers that support the diagnosis of CG are gastrin and pepsinogen. These are derived from gastric fluid and blood, respectively. The diagnostic procedure is invasive and uncomfortable, which precludes its use in some elderly patients and patients with coronary heart disease. Consequently, it is difficult to implement on a large scale.[6] The observation of tongue coating is a crucial diagnostic indicator in the identification of CG by traditional Chinese medicine (TCM) practitioners.[7] The diverse range of colours and thicknesses observed in the gastric mucosa correspond to the various causes of gastric disorders,[8,9] Dampness is one of the most prevalent forms of chronic gastritis, and according to WHO international standard terminologies on traditional Chinese medicine it can be classified into two categories: cold dampness pattern and damp heat pattern.[10] The distinction in tongue coating is a crucial factor in the differentiation of damp heat and cold dampness patterns. The tongue coating is a complex structure that is attached to the tongue and consists of a variety of components, including shed epithelial cells, blood cells, metabolites, nutrients, and bacteria.[11] The low cost, non-invasive, and safe collection of tongue moss offers a promising avenue for clinical diagnosis.[12] A previous study conducted by our research team identified the presence of differential metabolites in the tongue moss of patients diagnosed with coronary artery disease and chronic renal failure, characterised by a damp phlegm pattern.[13] The results of these studies indicate that tongue metabolites may be employed as a supplementary diagnostic tool for the identification of diseases.[14]

Metabolomics, as a branch of systems biology, is the study of qualitative and quantitative dynamic changes of metabolites in biological systems following disturbance by various factors. The role of gene expression, protein regulation, and other factors in complex signalling pathways can be elucidated through the end-product analysis of metabolomics. From the perspective of Chinese medicine, metabolomics regards the human body as a whole system.[15] The multidimensional observation of metabolomics can be utilised to conduct accurate comparative studies in the case of the same disease with different symptoms. In conclusion, metabolomics aligns with the precise thinking of TCM evidence-based treatment, and there is a promising avenue for studying the diverse patterns of chronic gastritis based on metabolomics. In a previous study, we employed metabolomics technology to identify metabolites in the tongues of patients with wet phlegm gastric precancerous lesions(GPL). Our findings indicated that the metabolite profiles of patients with damp phlegm GPL differed significantly from those of non-damp phlegm patients. Other studies have employed liquid chromatography and mass spectrometry (LC-MS) techniques to detect and analyse substances in the tongue moss of patients with chronic gastritis.[16,17] The differential metabolites in question may be utilised as potential markers for the monitoring of the onset and progression of chronic gastritis.

Given the limitations of current studies on tongue CG and the necessity for clinical diagnosis, the results obtained by using only one assay may be limited. In order to overcome these limitations, the present study combined UHPLC-QE-MS and GC-TOF-MS to perform a comprehensive metabolomics study. This was conducted using two different columns in positive and negative ion modes, respectively. This approach was employed to identify small molecules that could serve as non-invasive and convenient diagnostic biomarkers, as well as differential metabolic pathways, with the aim of constructing differential diagnostic models for the two CG groups.

Materials and Methods

Study Participants

A total of 200 CG patients were recruited for the study. A gastroscopy was conducted in CG patients immediately following the collection of their tongues, with the objective of recording both gastroscopic images and pathological indicators. The tongue metabolites of 200 subjects in the CG wet evidence group were analysed, including the CG cold-dampness evidence group (N=100) and the CG damp-heat evidence group (N=100). Subsequently, 18 clinical samples (including 3 cases of cold-dampness and 15 cases of damp-heat certificates) were randomly collected at a later stage to validate the diagnostic model.

The inclusion criteria were endoscopy and biopsy from suspected lesions (eg, gastric antrum and cardia). The histopathologic evaluation was completed by two experienced pathologists according to the clinical guidelines of the "Updated Sydney System".[18] The diagnosis of CG is based on two distinct procedures: diagnostic gastroscopy and diagnostic histopathology. These procedures are conducted in order to exclude patients who have previously undergone gastric polypectomy, gastric haemorrhage, gastric tumour resection, or specific gastritis.

The diagnostic criteria of the cold dampness and damp heat groups were primarily based on the Consensus Opinions on Integrative Diagnosis and Treatment of Chronic Gastritis, formulated by the Committee of Digestive Diseases of the Chinese Society of Integrative Medicine, and the Guidelines for Clinical Research of New Traditional Chinese Medicines, issued by the Ministry of Health. The final diagnosis was reached by consensus between two senior TCM experts with senior professional titles.

Basic Information About Sample Source

A summary of the clinical information and demographics of the participants is presented in Table 1. The study included 200 patients who were treated at Longhua Hospital Affiliated to Shanghai University of Traditional Chinese Medicine between 2018 and 2020. Prior to the commencement of the study, informed consent was obtained from all patients. The cold-dampness pattern group comprised 100 cases, with a male-to-female ratio of 1:1.33 and an average age of 50.73±15.17 years. The heat-dampness pattern group comprised 100 cases (male: female ratio of 1:1), with an average age of 48.88±13.75 years. There was no statistically significant difference in gender or age between the two groups ($P>0.05$). With regard to treatment, 37 individuals did not adhere to medical advice (16 cases of cold-dampness pattern, 21 cases of heat-dampness pattern). The remaining 163 individuals were treated with Western medicine or traditional Chinese medicine. Among the treated cases, 30 cases of cold-dampness pattern and 25 cases of heat-dampness pattern were treated with proton pump inhibitors and other Western medicines; 26 cases of dampness pattern and 25 cases of heat-dampness pattern were treated with traditional Chinese medicine. Furthermore, 28 patients with a dampness pattern and 29 patients with a heat-dampness pattern were treated with an integrated approach combining traditional Chinese and Western medicine.

Tongue Coating Samples Collection and Handling

Samples were collected in accordance with specific procedures. Prior to sampling, subjects were required to fast and refrain from tongue brushing for a minimum of six hours. At the time of collection, the tongue was rinsed with saline, swabbed several times with sterile medical swabs, with a minimum of two swabs per sample, and then placed into sterilised 5 mL EP tubes. Subsequently, the samples were stored in a refrigerator at a temperature of −80°C in order to prevent deterioration and degradation.

Reagents and Materials

The principal apparatus and reagents employed in the GC-TOF-MS and UHPLC-QE-MS assays are outlined in the Supplementary Materials.

Table 1 Summary of Demographics and Clinical Information of the Participants

Demographics and Clinical Information	Cold Dampness Pattern Group	Damp Heat Pattern Group
Sample number	100	100
Ratio of male to female	1: 1.33	1: 1
Average age (year)	50.73±15.17	48.88±13.75
Number (percentage) of samples diagnosed for less than 10 years	75 (75%)	75 (75%)
Number (percentage) of samples diagnosed for 10–20 years	7(7%)	16 (16%)
Number (percentage) of samples diagnosed for 20–30 years	9 (9%)	5 (5%)
Number (percentage) of samples diagnosed for 30–40 years	7 (7%)	3 (3%)
Number (percentage) of samples diagnosed over 40 years	2(2%)	1 (1%)
Number (percentage) of samples with helicobacter pylori infection	12 (12%)	9 (9%)
Number (percentage) of samples untreated	16 (16%)	21 (21%)
Number (percentage) of samples only taking western medicine (Taking prazole drugs.)	30 (30%)	25 (25%)
Number (percentage) of samples only taking traditional Chinese medicine	26 (26%)	25 (25%)
Number (percentage) of samples taking western medicine and traditional Chinese medicine	28 (28%)	29 (29%)

GC-TOF-MS/UHPLC-QE-MS Metabolomics Processing

As shown in Figure 1, the procedure for extracting metabolites for GC-TOF-MS analysis is outlined below. The process begins with sample extraction, followed by sonication in an ice-water bath, centrifugation, mixing, vacuum drying, oven incubation, cooling, the addition of FAMEs, and finally, the on-board assay.

As shown in Figure 2, The UHPLC-QE-MS assay metabolite extraction process is briefly described as follows: sample extraction, vortex mixing, and ultrasonic ice water bath. The samples were maintained at a temperature of −40°C. Centrifugation is then performed. The subsequent stage of the process is the detection of the metabolites on the machine.

GC-TOF-MS/UHPLC-QE-MS Conditions

GC-TOF-MS detection was performed utilising an Agilent 7890 gas chromatography-time-of-flight mass spectrometer, equipped with an Agilent DB-5MS capillary column (30m×250μm×0.25μm, J&W Scientific, Folsom, CA, USA) for the samples. The specific analytical conditions for the GC-TOF-MS are detailed in Table 2. The GC-TOF-MS experimental instrument list and the experimental reagent list are listed in (Supplementary Materials 1 and 2).

The UHPLC-QE-MS assay was conducted by chromatographic separation of the target compounds on a Waters ACQUITY UPLC BEH Amide (2.1 mm × 100 mm, 1.7 μm) liquid chromatography column using a Vanquish (Thermo Fisher Scientific)

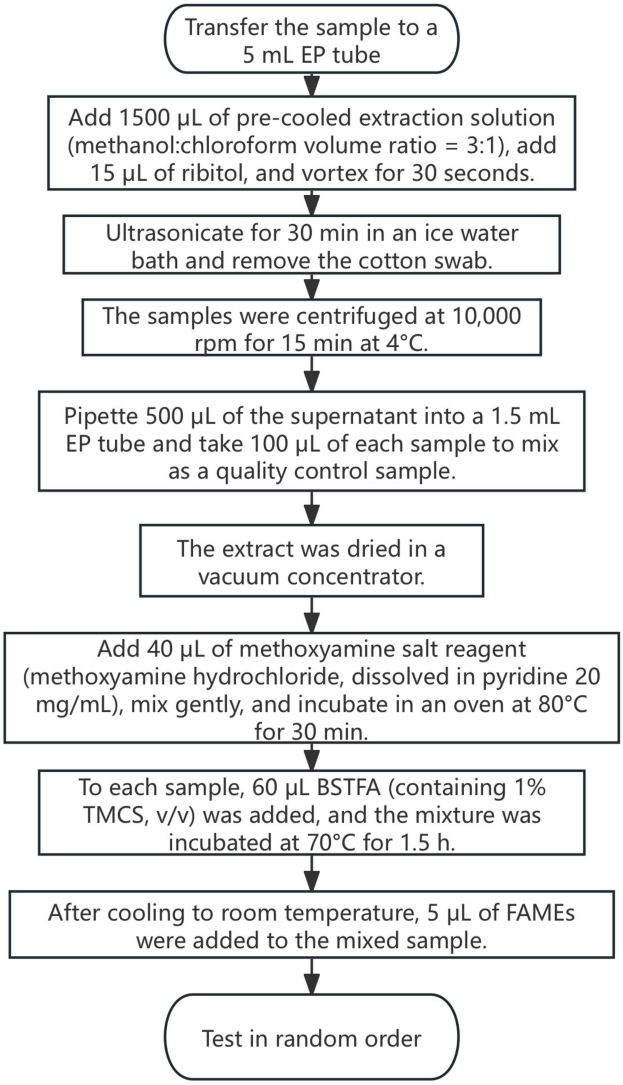

Figure 1 The procedure for extracting metabolites for GC-TOF-MS analysis.
Abbreviations: BSTFA, N,O-Bis(trimethylsilyl)trifluoroacetamide; TMCS, Chlorotrimethylsilane; FAMEs, Fatty Acid Methyl Ester Mass Spectral Library.

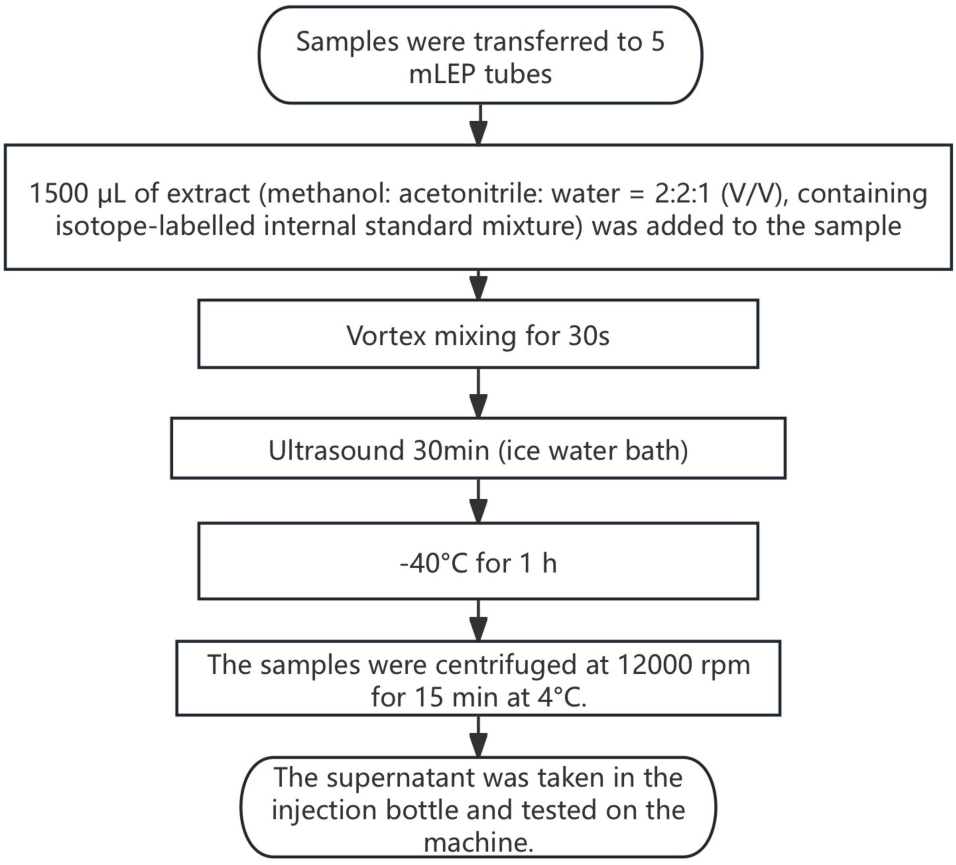

Figure 2 The procedure for extracting metabolites for UHPLC-QE-MS analysis.

ultra-high performance liquid chromatograph (UPLC). The liquid chromatographic phase A consisted of an aqueous solution containing 25 mmol/L ammonium acetate and 25 mmol/L ammonia, while phase B was acetonitrile. A gradient elution method was employed. The gradient elution programme commenced at 0 minutes and 0.5 seconds, with a composition of 95% B. This was followed by a transition to 95% B to 65% B over a period of 0.5 to 7 minutes. The composition then changed to 65% B to 40% B over a period of 7 to 8 minutes. This was then followed by a transition to 40% B over a period of 8 to 9 minutes. The composition then changed to 40% B to 95% B over a period of 9 to 9.1 minutes. Finally, the composition returned to 95% B over a period of 9.1 to 12 minutes. The flow rate of the mobile phase was 0.5 mL/min, the temperature of the column was 25°C, and the temperature of the sample tray was 4°C. The temperature was maintained at 4°C, with an injection volume of 3 μL. The specific parameters are presented in Table 3. The UHPLC-QE-MS experimental instrument list and the experimental reagent list are listed in (Supplementary Materials 3 and 4).

Table 2 Instrument Parameters

Program	Parameter
Sample Volume	1μL
Front Inlet Mode	Splitless Mode
Front Inlet Septum Purge Flow	3mL/min
Carrier Gas	Helium
Column	DB-5MS (30m×250μm×0.25μm)
Column Flow	1mL/min
Oven Temperature Ramp	50°C hold on 1min, raised to 310°C at a rate of 20°C/min, hold on 6min
Front Injection Temperature	280°C
Transfer Line Temperature	280°C

https://doi.org/10.2147/JIR.S480405

Table 3 Instrument Parameters

Program	POS	NEG
Spray voltage	3.5 kV	−3.2 kV
Capillary temperature	320°C	320°C
Sheath gas flow rate	50Arb	50Arb
Aux gas flow rate	10Arb	10Arb
Full ms resolution	60000	60000
MS/MS resolution	7500	7500
NCE/stepped NCE	10,30,60	10,30,60

Abbreviations: POS, UHPLC-QE-MS positive ion mode analysis mode; NEG, UHPLC-QE-MS negative ion mode analysis mode.

The Thermo Q Exactive HFX mass spectrometer is capable of acquiring both primary and secondary mass spectrometry data under the control of the Xcalibur software, developed by Thermo.

Data Processing and Analysis

As shown in Figure 3, Metabolomics data preprocessing and analysis were performed using SIMCA software (version 15.0.2, Sartorius Stedim Data Analytics AB, Umeå, Sweden). Raw data were subjected to logarithmic (LOG) transformation and unit variance (UV) scaling. An orthogonal partial least squares-discriminant analysis (OPLS-DA) model was constructed based on the first principal component. Model validity was evaluated using 7-fold cross-validation, with interpretability (R^2Y) and predictability (Q^2) metrics. Permutation testing (200 iterations) was further applied to verify robustness by randomly shuffling the categorical variable Y and comparing the resultant Q^2 values with the original model.

Differential metabolites were screened using the following criteria: Statistical significance (Wilcoxon rank-sum test, $P< 0.05$); Variable importance in the projection (VIP) score > 1 from the OPLS-DA first principal component; GC-TOF-MS similarity value (SV) > 70; UHPLC-QE-MS MS2 spectral match score > 0.5.

Hierarchical clustering of differential metabolites was conducted using a Euclidean distance matrix and complete linkage method. Kyoto Encyclopedia of Genes and Genomes (KEGG) Pathway database (http://www.kegg.jp/kegg/pathway.html) was utilized to map human (Homo sapiens) metabolic pathways associated with the identified metabolites. Key pathways were prioritized through combined enrichment analysis and topological evaluation.

To assess diagnostic potential, receiver operating characteristic (ROC) curves were generated for all metabolite combinations. The optimal diagnostic model was selected based on the highest area under the curve (AUC) value.

Results

Preparation and Organization of Raw Data

In order to ensure the reliability of the data, a series of preparatory and organisational measures were implemented on the original data. The main steps involved in this process are as follows: the individual mass spectrum peaks are filtered in order to remove any noise. Outliers were identified based on the interquartile range. The individual mass spectral peaks were then subjected to filtration. Only peak area data with no more than 50% null values in a single group or no more than 50% null values in all groups are retained. It is necessary to simulate the missing values in the original data. The numerical simulation method fills in half the minimum value. The data underwent standardisation processing. The total ion current was employed as the normalization factor for each sample.

Mass Spectrum

As shown in Figure 4, the GC-TOF-MS analysis mass spectrum of a randomly selected sample from each of the CG cold dampness pattern group and CG damp heat pattern group is presented. Figure 5 depicts the UHPLC-QE-MS positive ion mode analysis mass spectrum, while Figure 6 presents a similar analysis mass spectrum.

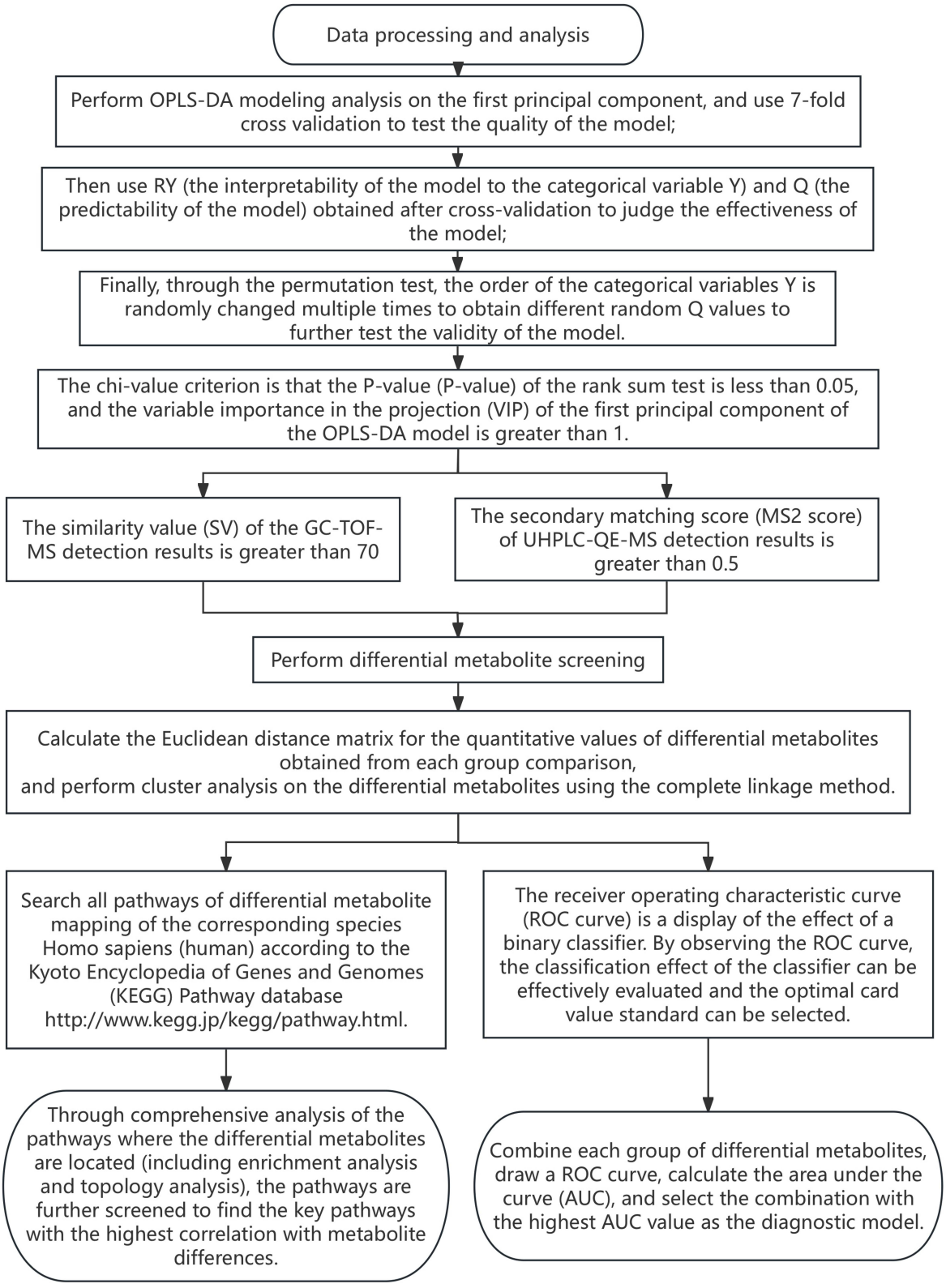

Figure 3 Data analysis Data analysis process.
Abbreviation: OPLS-DA, Orthogonal partial least squares discriminant analysis.

https://doi.org/10.2147/JIR.S480405

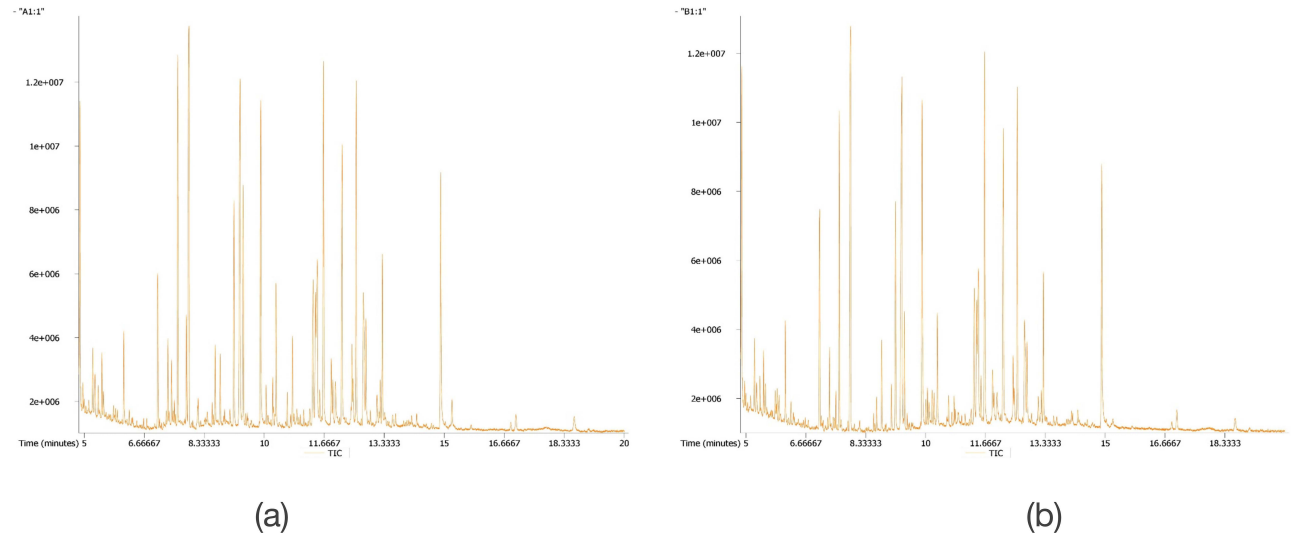

Figure 4 GC-TOF-MS mode analysis mass spectrum. (**a**) CG cold dampness pattern group. (**b**) CG damp heat pattern group.

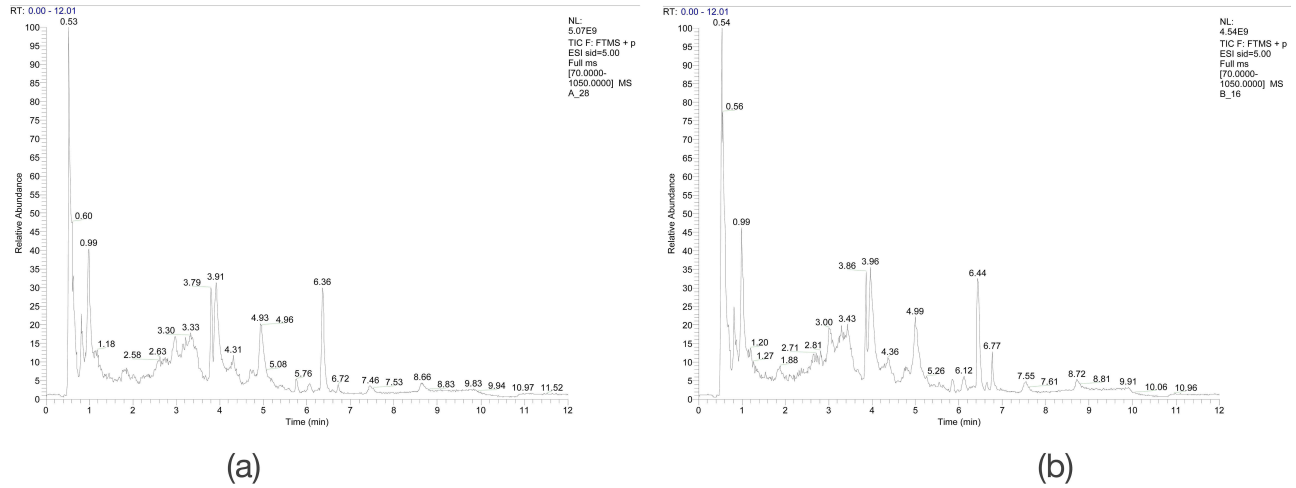

Figure 5 UHPLC-QE-MS positive ion mode analysis mass spectrum. (**a**) CG cold dampness pattern group. (**b**) CG damp heat pattern group.

The Reliability of the Data

As shown in Figure 7, the OPLS-DA score chart for GC-TOF-MS, UHPLC-QE-MS positive ion mode, and UHPLC-QE-MS negative ion mode. The samples belonging to the cold dampness pattern group and the damp heat pattern group were found to be significantly different, with the samples falling within the 95% confidence interval.

The results of the permutation test for the OPLS-DA model are presented in Figure 8. The GC-TOF-MS model (R^2 Y = 0.507, Q^2 = −0.183) and the UHPLC-QE-MS positive ion mode (R^2 Y = 0.460, Q^2 = 0.188), UHPLC-QE-MS negative ion mode (R^2 Y = 0.535, Q^2 = 0.131) exhibited robust performance and did not exhibit overfitting.

Differential Metabolites Analysis

GC-TOF-MS Detection

The Chi-value criterion is that the P-value of the rank sum test is less than 0.05, the variable importance in the projection (VIP) of the first principal component of the OPLS-DA model is greater than 1, and the GC-TOF-MS detection result's similarity value (SV) is greater than 70. It is necessary to perform differential metabolite screening.

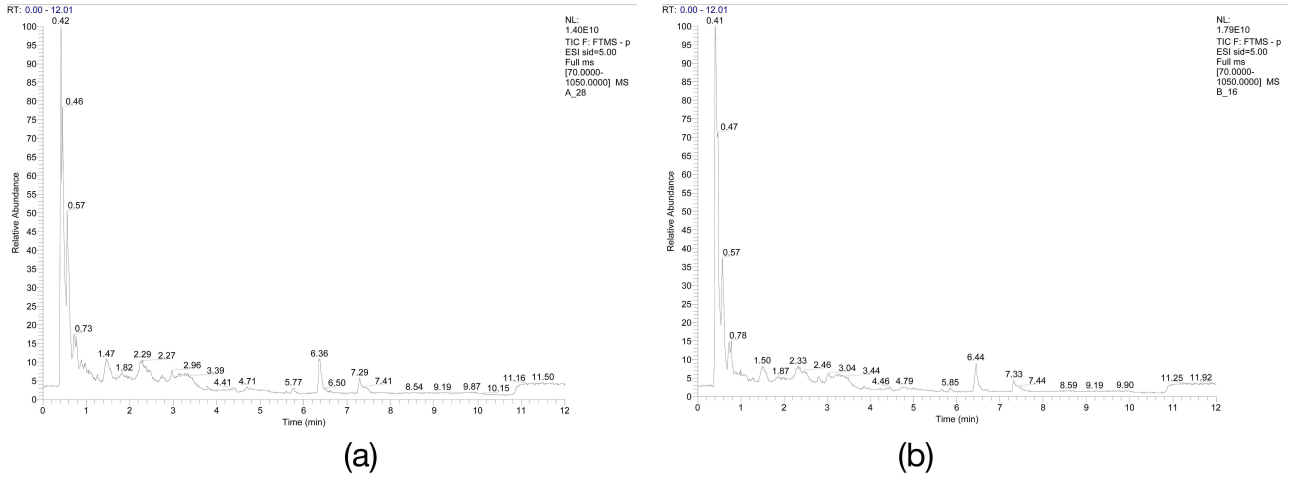

Figure 6 UHPLC-QE-MS negative ion mode analysis mass spectrum. (**a**) CG cold dampness pattern group. (**b**) CG damp heat pattern group.

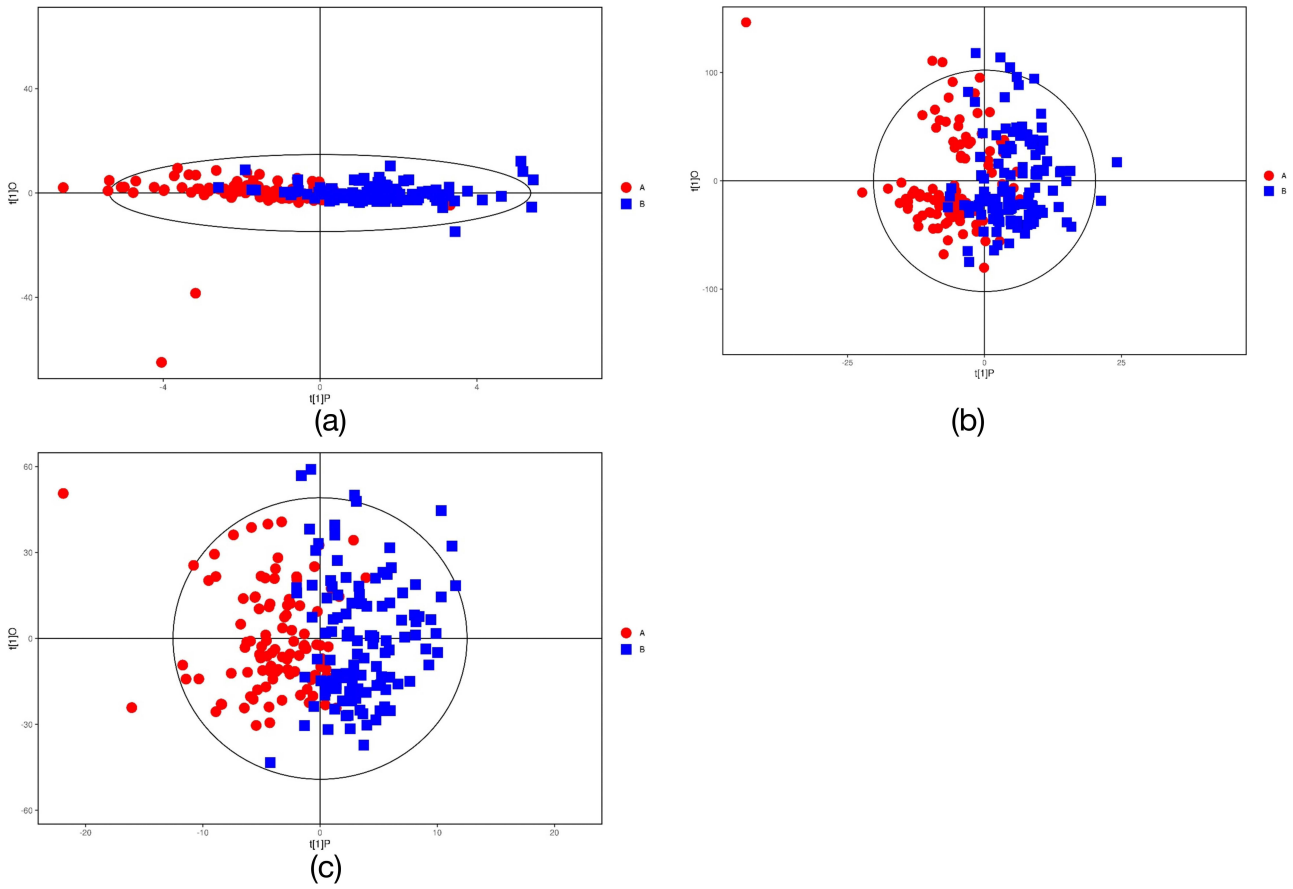

Figure 7 OPLS-DA model score scatter plot. (**a**) the OPLS-DA scoring charts of GC-TOF-MS; (**b**) the OPLS-DA scoring charts of UHPLC-QE-MS positive ion mode; (**c**) the OPLS-DA scoring charts of UHPLC-QE-MS negative ion mode. A(red): CG cold dampness pattern group. B(blue): CG damp heat pattern group.

As shown in Table 4, The GC-TOF-MS test results, based on the appeal conditions, revealed the presence of three known metabolites that exhibited significant differences between the CG cold-dampness pattern group and the CG damp-heat pattern group. Among the metabolites, fucose 1 and 4-hydroxybenzoate were found to be significantly upregulated, while phenol was significantly downregulated in the CG cold-dampness pattern group.

https://doi.org/10.2147/JIR.S480405

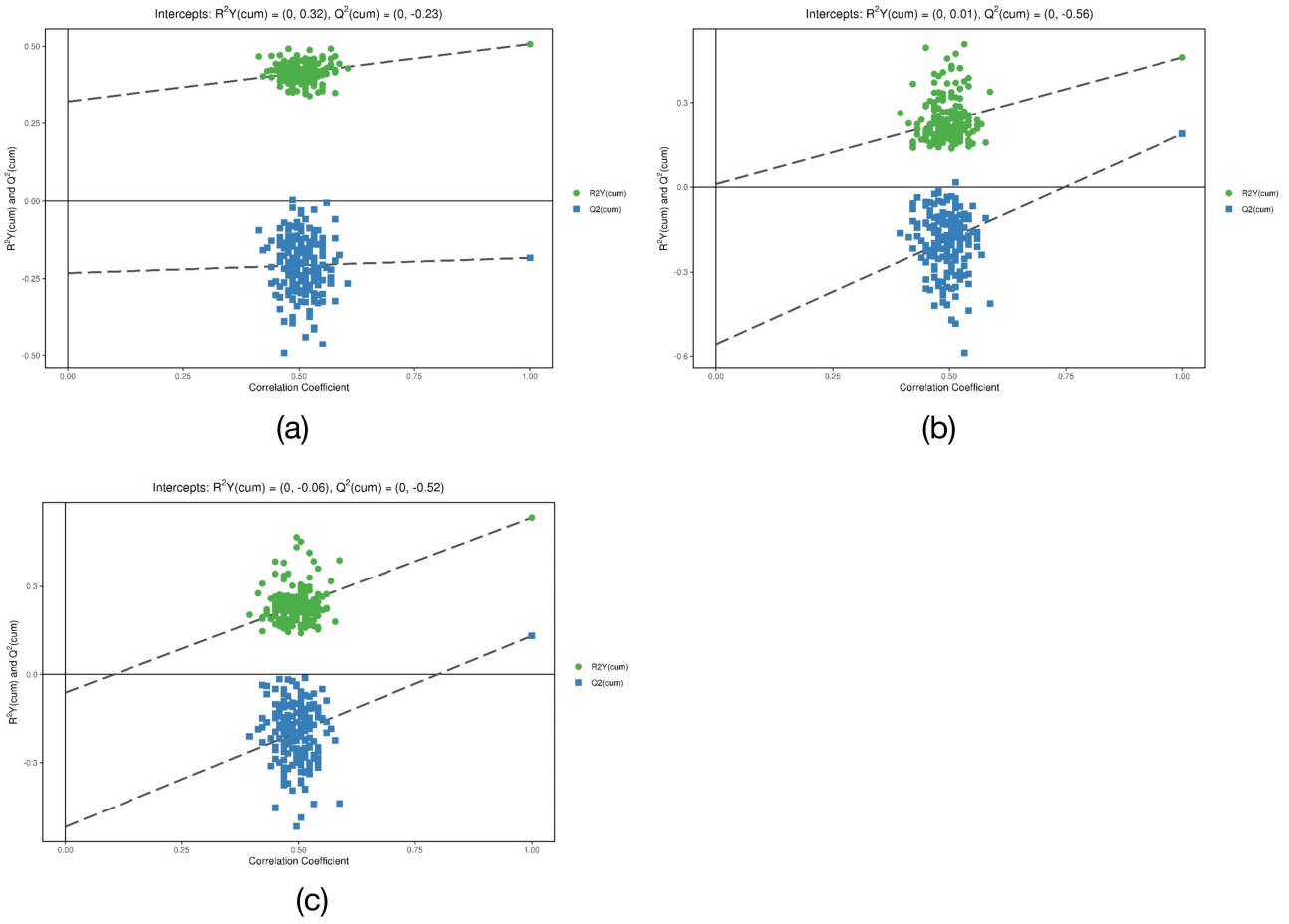

Figure 8 Permutation test plot of OPLS-DA model. (**a**) The permutation test results of the OPLS-DA model of GC-TOF-MS; (**b**) The permutation test results of the OPLS-DA model of UHPLC-QE-MS positive ion mode; (**c**) The permutation test results of the OPLS-DA model of UHPLC-QE-MS negative ion mode.

UHPLC-QE-MS Detection

The chi-value criterion is that the P-value of the rank sum test is less than 0.05, the variable importance in the projection (VIP) of the first principal component of the OPLS-DA model is greater than 1, and the secondary matching score (MS2 score) of the test results is greater than 0.5 for differential metabolite screening.

As shown in Table 5, the UHPLC-QE-MS positive ion mode analysis mode was subjected to screening based on the appeal conditions, and it was determined that 13 known metabolites exhibited significant differences between the CG cold-damp pattern group and the CG damp-heat pattern group. These metabolites belonged to three distinct categories: organic nitrogen compounds, lipids, and lipids, respectively. In addition to the aforementioned molecules, organic oxygen compounds, benzene ring compounds, organic sulfur compounds, phenylpropanoids and polyketides were also identified.

Table 4 Differential Metabolites in the GC-TOF-MS Detection Results Compared Between the CG Cold-Damp Pattern Group and the CG Damp-Heat Pattern Group

Metabolite Name	RT (min)	M/Z	Cold-Damp Pattern	Damp-Heat Pattern	*P*	VIP	Log Fold Change
Phenol	5.536	151	0.005	0.007	<0.01	1.358	0.615
Fucose 1	10	117	7.002E-04	5.758E-04	0.039	2.473	1.216
4-hydroxybenzoate	9.423	110	0.062	0.057	<0.01	1.426	1.091

Abbreviations: RT (min), Retention Time (minutes); M/Z, Mass-to-Charge Ratio; *P*, p-value; VIP, Variable Importance in Projection; Log fold change, Logarithmic Fold Change.

Table 5 Differential Metabolites Compared Between the CG Cold-Damp Pattern Group and the CG Damp-Heat Pattern Group Under UHPLC-QE-MS Positive Ion Mode Analysis Mode

Metabolite Name	RT (Min)	M/Z	Cold-Damp Pattern	Damp-Heat Pattern	*P*	VIP	Log Fold Change
Organic nitrogen compounds							
1-Butylamine	268.847	74	12.144	13.199	<0.01	3.394	0.920
Octadecylamine	85.691	270	0.410	0.184	0.031	1.633	2.228
Phytosphingosine	61.205	318	31.426	41.578	<0.01	2.552	0.756
Lipids and lipid-like molecules							
(1(10)E,4E,6a,9b)-9-(2-Methylbutanoyloxy)-1(10),4,11(13)-germacratrien-12,6-olide	106.492	333	0.107	0.130	0.025	1.762	0.823
Lactosylceramide (d18:1/26:0)	31.388	1003	0.005	0.003	<0.01	1.973	2.052
Phosphatidylethanolamine	165.917	646	0.378	0.312	0.027	1.978	1.210
Organic oxygen compounds							
3-Dehydrophingosine	166.001	300	0.074	0.134	<0.01	1.604	0.554
Benzene ring compound							
Alpha Methystyrene	36.149	119	2.489	3.753	<0.01	1.327	0.663
Organosulfur compounds							
(Â±)-2-Pentanethiol	32.769	105	0.395	0.439	<0.01	2.402	0.900
Phenylpropanoids and polyketides							
7-Hydroxy-5-methoxy-6,8-dimethyllavenone	152.657	299	0.005	0.005	0.025	1.255	0.942
Other							
PA(18:2(9Z,12Z)/16:1(9Z))	186.137	671	0.960	0.865	0.032	1.103	1.110
1,4'-Bipiperidine-1'-carboxylic acid	47.858	213	0.625	0.672	0.021	2.935	0.931
PE(P-16:0/16:1(9Z))	163.487	674	1.347	1.213	0.045	2.096	1.112

In the CG cold dampness pattern group, Octadecylamine, Lactosylceramide (d18:1/26:0), PA (18:2 (9Z, 12Z)/16:1 (9Z)), PE (P-16:0/16:1 (9Z)), and phosphatidylethanolamine are significantly upregulated, 1-Butylamine, Phytosphingosine, (1 (10) E, 4E, 6a, 9b) −9- (2-Methylbertanoyloxy) −1 (10), 4,11 (13) - gemaratien-12,6-olide, 3-Dehydrophingosine, alpha Methystyrene, (Â±)-2-Pentanethiol, 7-Hydroxy-5-methoxy-6,8-dimethyllavenone, 1,4 "- Piperidine-1" - carboxylic acid are significantly downregulated.

As shown in Table 6, the UHPLC-QE-MS negative ion mode analysis mode was subjected to screening according to the appeal conditions, and it was found that there were significant differences in four known metabolites between the CG cold-dampness pattern group and the CG damp-heat pattern group. These metabolites belong to the categories of lipids and steroids, respectively. The identified metabolites were classified as lipid molecules, benzene ring compounds, organic acids and their derivatives. Among the metabolites, 4-Dodecylbenzenesulfonic Acid and Ketoleucine were found to be significantly upregulated, while Caprylic acid and 6beta-Hydroxyasiatic acid were significantly downregulated in the CG cold-damp pattern group.

Differential Metabolic Pathway Analysis

A search was conducted of all pathways corresponding to the species Homo sapiens (human) differential metabolite mapping according to the KEGG database. A comprehensive analysis of the pathways where the differential metabolites

Table 6 Differential Metabolites Compared Between the CG Cold-Damp Syndrome Group and the CG Damp-Heat Syndrome Group Under UHPLC-QE-MS Negative Ion Mode Analysis Mode

Metabolite Name	RT (Min)	M/Z	Mean Damp Phlegm Pattern	Mean Non-Damp Phlegm Pattern	*P*	VIP	Log Fold Change
Lipids and lipid molecules							
Caprylic acid	50.617	143	2.808	3.205	0.040	1.048	0.876
6beta-Hydroxyasiatic acid	51.604	503	0.126	0.141	<0.01	2.001	0.897
Benzene ring compound							
4-Dodecylbenzenesulfonic Acid	27.792	325	5.496	3.818	<0.01	2.194	1.439
Organic acids and their derivatives							
Ketoleucine	197.903	129	0.367	0.308	<0.01	1.728	1.191

Table 7 Differential Metabolic Pathways Compared Between CG Cold-Damp Syndrome Group and CG Damp-Heat Syndrome Group

Pathway	Raw p	Impact	Significantly Different Metabolites
UHPLC-QE-MS positive ion mode analysis			
Glycerophospholipid metabolism	0.063	0.128	Phosphatidylethanolamine
Sphingolipid metabolism	3.936E-06	0.064	Phytosphingosine, 3-dehydrosphingosine, lactosylceramide
Glycosylphosphatidylinositol(GPI)-anchored biosynthesis	0.023	0.044	Phosphatidylethanolamine

Abbreviation: Raw p, Raw p-value.

are located (including enrichment analysis and topology analysis) is conducted to identify the key pathways with the highest correlation with metabolite differences.

As shown in Table 7, the UHPLC-QE-MS positive ion mode analysis revealed that, in comparison to the CG cold-damp pattern group and the CG damp-heat pattern group, there were four differential metabolites involved in three metabolic pathways, namely glycerophospholipid metabolism and sphingolipid metabolism, and glycosylphosphatidylinositol (GPI)-anchored biosynthesis.

Diagnostic Model

The diagnostic model was constructed by screening the differential metabolites of tongue coating in 100 cases of CG cold-dampness syndrome and 100 cases of CG damp-heat syndrome. The best diagnostic model was finally obtained, which was composed of phenol screened by GC-TOF-MS. Compared with CG damp-heat syndrome, phenol was significantly downregulated in CG cold-dampness syndrome. The tongue coating metabolites of 18 CG patients (including 3 cases of cold-dampness pattern and 15 cases of damp-heat pattern) were randomly tested clinically to verify the model. As can be seen from the ROC curve (Figure 9), the accuracy of the diagnostic model was 80.0%, the specificity was 100.0%, and the sensitivity was 73.3%.

Discussion

The rapidly evolving field of metabolomics holds transformative potential across three critical dimensions of modern healthcare: Metabolomic profiling enables the identification of disease-specific metabolic signatures long before clinical symptoms manifest. For instance: In oncology, aberrant sphingolipid metabolism has been detected 5–8 years prior to

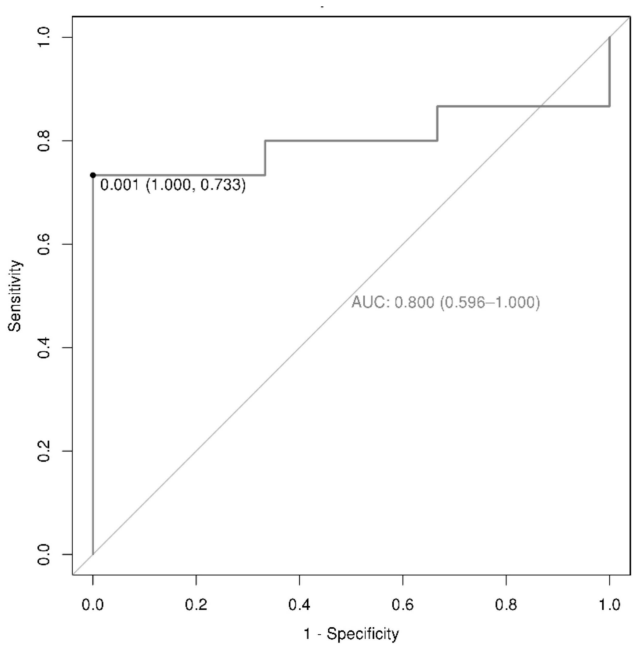

Figure 9 ROC curve of the diagnostic model of CG cold-dampness syndrome and CG damp-heat syndrome.

pancreatic cancer diagnosis.[19] Neurodegenerative disease prediction through CSF kynurenine pathway metabolites shows 89% specificity for Alzheimer's progression.[20] Real-time metabolic tracking revolutionizes therapeutic management: Chemotherapy response can be assessed within 48 hours via serum lactate/pyruvate ratios.[21] Diabetic nephropathy progression is quantifiable through urinary acylcarnitine trajectories.[22]

As more and more researchers join in, it is worth affirming that tongue coating metabolites have many clinical values worth exploring. A multicenter study used pressure cycling technology and data-independent acquisition (PCT-DIA) mass spectrometry to extract and identify tongue coating proteins from 180 gastric cancer patients and 185 non-gastric cancer patients from 5 independent research centers in China, and used the stochastic gradient boosting algorithm to build a machine learning model that used 50 tongue coating microbial proteins to identify individuals at high risk of gastric cancer, achieving an area under the curve (AUC) of 0.91 in an independent validation cohort.[23]

GC-TOF-MS and UHPLC-QE-MS have distinct advantages in metabolite analysis. In polar metabolite analysis, GC-TOF-MS exhibits a greater degree of separation power than UHPLC-QE-MS. Nevertheless, GC-TOF-MS is capable of detecting approximately 100 metabolites, whereas UHPLC-QE-MS can detect thousands of metabolites, including semipolar metabolites.[24] The composition of metabolites on the tongue coating is complex, and thus the combined use of two detection methods can provide a more comprehensive understanding of the characteristics of metabolites on the tongue coating.[25]

Metabolic alterations in specimens can serve as a biochemical foundation for the etiology and progression of disease.[26] This study employed GC-TOF-MS and UHPLC-QE-MS metabolomics technologies to identify metabolites in the tongue coating of CG patients. This approach enabled the detection of 16 differential biomarkers, including lipids and lipid molecules, organic nitrogen compounds, benzene ring compounds, organic acids and their derivatives, organic oxygen compounds, organic sulfur compounds, and other categories.

The research findings indicate that lipids and lipid-like molecules represent the most diverse group. A comparison of lipid metabolites between the CG cold-dampness pattern group and the CG damp-heat pattern group revealed that: The CG cold-dampness pattern group exhibited significant upregulation of 4-hydroxybenzoate, lactosylceramide (d18:1/26:0), and phosphatidylethanolamine (1(10)E,4E,6a,9). In contrast, (1(10)E,4E,6a,9b)-9-(2-Methylbutanoyloxy)-1-(10),4,11(13)-germacratrien-12,6-olide, octanoic acid, and 6β-hydroxyasinic acid exhibited a significant downregulation.

Lipid metabolites are essential components of the human body, serving as a source of energy through beta-oxidation and constituting a significant portion of cell membranes,[27,28] A number of studies have indicated that lipid metabolism

plays a role in the progression of gastric cancer (GC).[29] Some studies have indicated that lipids may play a role in the development of chronic atrophic gastritis.[30] Chronic gastritis is associated with an overall increase in the body's inflammatory state, which is affected by adverse lipid status. This includes a decrease in serum high-density lipoprotein (HDL), which is closely associated with an increased risk of gastric cancer,[31,32] Concurrently, research has demonstrated that aberrant lipid metabolism can precipitate a cascade of inflammatory responses. Patients with hyperlipidaemia will exhibit long-term systemic inflammation, and serum inflammatory factor levels will also increase in parallel with the elevation of blood lipid levels.[33] Furthermore, studies on mice have indicated that a diet high in cholesterol and fat may increase the prevalence of gastritis in mice.[34] It is also worth noting that disorders of lipid metabolites occur in gastric cancer patients. Studies have demonstrated that rapidly proliferating cancer cells are capable of survival through the enhancement of exogenous lipid uptake and the activation of endogenous lipid synthesis, which serves to provide energy. Consequently, the serum of gastric cancer patients exhibits an upregulation of lipid metabolite levels.[35]

Ceramide and sphingosine are negative regulators of cell proliferation, inhibiting cell growth and promoting apoptosis.[36] In this study, the differential metabolites screened out by comparing the cold-dampness pattern group and the damp-heat pattern group were phytosphingosine, 3-dehydrosphingosine, and lactosylceramide (d18:1/26:0 in the cold-dampness group). The three types of metabolites exhibited a downward trend. The higher level of sphingosine observed in the tongue coating of CG patients in the damp-heat group compared to the cold-damp group suggests that apoptosis of tongue epithelial cells may be accelerated in the former group. The number of other differential metabolites is fewer, and studies have demonstrated that the mitotic index declines with increasing paraben concentration. The results demonstrated that methylparaben and ethylparaben induce an increased frequency of apoptosis.[37] The theory of traditional Chinese medicine posits that the greasy coating of the cold-dampness pattern is the result of the accumulation of dampness and turbidity, the suppression of Yang Qi, and the accumulation of dampness and phlegm on the tongue surface.[38] The upregulation of 4-hydroxybenzoate in the cold-dampness group indicated that the frequency of apoptosis of tongue coating cells in this group of patients increased, thereby revealing the formation mechanism of the greasy coating. It has been demonstrated that caprylic acid can enhance lipid metabolism and suppress the inflammatory response in rats.[39,40]

The analysis of metabolic pathways of lipids and lipid-like molecules revealed the involvement of three metabolic pathways: glycerophospholipid metabolism, sphingolipid metabolism, and glycosylphosphatidylinositol (GPI)-anchored biosynthesis. The metabolic pathway is comprised of four differential metabolites: phosphatidylethanolamine, phytosphingosine, 3-dehydrosphingosine, and lactosylceramide.

Among the aforementioned phospholipids, phosphatidylethanolamine plays a role in glycerophospholipid metabolism. Phospholipids represent the principal constituents of cell membranes, and lipid metabolism plays a pivotal role in maintaining cell membrane homeostasis.[41] In physiological conditions, polyunsaturated fatty acids (PUFAs) undergo esterification catalysed and mediated by a series of enzymes, combining with phosphatidylethanolamines (PEs) on the cell membrane to form PUFA-PEs, which causes membrane structural instability. The degree of saturation increases. PUFA-PE is a pivotal substrate for the induction of ferroptosis, and its concentration exerts a significant influence on the ferroptosis susceptibility of cells.[42] The results of these studies indicate that disorders of glycerophospholipid metabolism involving phosphatidylethanolamine may be involved in the pathogenesis of chronic gastritis by inducing ferroptosis. Previous studies have indicated a potential association between ferroptosis and inflammation.[43] It is important to highlight that the three principal pathways involved in the occurrence and development of ferroptosis are iron metabolism, lipid metabolism and amino acid metabolism. The analysis of tongue coating metabolites with regard to iron metabolism has not yet been addressed. This study identified differential metabolites in the tongue coating. From the analysis of lipid metabolism pathways, it can be inferred that there may be a certain connection between chronic gastritis and ferroptosis in the metabolomics of the tongue coating. This warrants further investigation in subsequent experiments.

Furthermore, studies have demonstrated that there are evident abnormalities in glycerophospholipid metabolism in gastrointestinal cancer. In patients with gastrointestinal cancer, the levels of phosphatidylcholines, lysophosphatidylcholines and sphingomyelin are significantly lower than those observed in the control group, while the levels of fatty acids and ketones are lower. Significantly higher than the normal group. The hydrolysis of glycerophospholipids in the body is a process catalysed by phospholipases within the body. Phospholipases are enzymes that catalyze the hydrolysis of ester bonds in glycerophospholipid molecules, resulting in the generation of lysophospholipids and unsaturated fatty acids,[44,45]

In addition to glycerophospholipid metabolism, phosphatidylethanolamine is also involved in the glycosylphosphatidylinositol-anchored biosynthetic pathway. It has been demonstrated that this metabolic pathway plays a role in stimulating the synthesis of lipids and glycogen between cells.[46]

The equilibrium of cellular sphingolipid metabolism is a crucial aspect of cellular homeostasis and also plays a pivotal role in the regulation of cell proliferation, differentiation, and apoptosis. The differential metabolites involved in sphingolipid metabolism in this study are phytosphingosine, 3-dehydrosphingosine, and lactosylceramide. It has been demonstrated that alterations in sphingolipid metabolism can influence the progression of cancer, the efficacy of treatment, and the prognosis,[47,48] Concurrently, the most significant alterations in the metabolites of the tongue coating in patients with GPL are observed in lipid metabolism, specifically in sphingolipid metabolism and arachidonic acid metabolism.[49] Sphingolipids, particularly ceramide (Cer) and sphingosine, play a pivotal role in regulating the growth and proliferation of tumour cells. The current research on Cer and sphingosine has primarily demonstrated that they inhibit cell growth and accelerate cell apoptosis.[50] A number of studies have demonstrated that Cer functions as a mediator that induces cell apoptosis. Furthermore, these studies have indicated that Cer can trigger both endogenous and exogenous cell apoptosis. Cer can participate in the apoptosis pathway induced by tumour necrosis factor (TNF) via the endoplasmic reticulum and mitochondrial pathways.[51] A number of studies have demonstrated that the tongue coating of CG patients exhibits abnormal proliferation, differentiation, apoptosis and shedding of tongue epithelial cells. It is postulated that the thickness of the tongue coating may be influenced by aberrant cell sphingolipid metabolism, which regulates cell apoptosis.

The annotations of significantly different metabolites in the KEGG database, as well as the results of enrichment analysis and topology analysis, based on the original p-value and impact value, indicate that glycerophospholipid metabolism is the most important metabolic pathway. The differential substitute involved is phosphatidylethanolamine. In our previous research, we found that when comparing patients with wet phlegm type GPL and non-wet type patients, the most important metabolic pathway was glycerophospholipid metabolism, with phosphatidylethanolamine and hemolytic PC (18:1 (9Z)) being the key metabolites. Of these, the levels of phosphatidylethanolamine, which is involved in the metabolism and synthesis of glycerophospholipids, were significantly increased in patients with wet phlegm GPL. The results of this experiment demonstrated that the level of phosphatidylethanolamine, which is involved in the metabolism and synthesis of glycerophospholipids in the CG cold-dampness pattern, was significantly increased. This indicates that the involvement of phosphatidylethanolamine in the metabolism of glycerophospholipids can be employed as a factor that is differentially expressed among different pattern groups in patients with CG dampness pattern. Significant metabolic pathways were identified.

Finally, we reviewed the content and results of this study and found that there are many deficiencies that deserve further prospect and exploration. While our metabolomic profiling has identified potential biomarkers, this study has three main limitations: The specific biological mechanisms underlying the dysregulated metabolites and their pathological roles in chronic gastritis remain to be fully elucidated. Despite external validation, the single-center design with limited sample size may constrain the generalizability of our diagnostic model compared to multicenter cohorts. The mono-omics approach restricts comprehensive understanding of disease pathophysiology, which inherently involves complex interactions across biological layers.

To address these limitations, we propose a three-phase roadmap: Establish multicenter cohorts incorporating transcriptomic, proteomic, and gut microbiome data to construct robust cross-omics diagnostic frameworks. Employ organoid models and genetically engineered mice to validate the causal relationships between candidate metabolites and disease progression. Implement machine learning pipelines for dynamic risk prediction, focusing on clinical deployment of biomarker panels through point-of-care testing devices.

As a pioneering exploration, this study establishes essential data infrastructure and methodological frameworks for advancing multi-omics diagnostics in gastrointestinal disorders. The identified metabolite signatures, while requiring further validation, provide actionable insights for developing precision medicine strategies in chronic gastritis management.

Conclusion

In conclusion, a metabolomics analysis method based on GC-TOF-MS and UHPLC-QE-MS was established, utilising both positive and negative ion modes to analyse the tongue coating of CG patients and healthy individuals. By measuring the

metabolic components of the tongue coating samples of the CG cold-damp pattern group and the CG damp-heat pattern group, it was found that there were significant differences in the metabolome of the two groups of patients. Ultimately, 20 metabolite biomarkers were identified through the screening process. Including fucose 1, 4-hydroxybenzene formate, phenol, octadecylamine, lactosylceramide (d18:1/26:0), PA(18:2(9Z,12Z)/16:1(9Z)), PE(P-16:0/16:1(9Z)), phosphatidylethanolamine, 1-Butylamine, phytosphingosine, (1(10)E,4E,6a,9b)-9-(2-Methylbutanoyloxy)-1(10),4,11(13)-germacratrien- 12,6-olide, 3-Dehydrosphinganine, alpha-Methylstyrene, (Â±)-2-Pentanethiol, 7-Hydroxy-5-methoxy-6,8-dimethylflavanone, 1,4'-Bipperidine-1'-carboxylic acid, 4-Dodecylbenzenesulfonic acid, Ketoleucine, Caprylic acid, 6beta-Hydroxyasiatic acid. Among the various types of lipids and lipid molecules, these are the most prominent. At the same time, three differential metabolic pathways were identified through metabolic pathway analysis of differential metabolites: glycerophospholipid metabolism, sphingolipid metabolism, and glycosylphosphatidylinositol (GPI)-anchored biology. Among the identified metabolic pathways, glycerophospholipid metabolism is of particular significance, with phosphatidylethanolamine serving as the key metabolite. Furthermore, ROC curve analysis was employed to identify the diagnostic model constructed by screening differential metabolites in tongue coating. Among the differential metabolites, the optimal diagnostic model was ultimately identified and comprised phenol, which was selected by GC-TOF-MS. In the future, it would be beneficial to combine the results of tongue coating metabolomics with those of proteomics, genomics, and transcriptomics in order to conduct a systematic and in-depth study of CG patients with different pattern types. The objective is to identify differential metabolites between different pattern types. It may prove to be a valuable diagnostic marker, offering the potential to provide diagnostic markers for the objective classification of different TCM CG patterns.

Ethics Statement

Prior to sample collection, all subjects were required to sign a written informed consent form. The study was conducted in accordance with the Declaration of Helsinki. Furthermore, this study was approved by the Ethics Committee of Shanghai University of Traditional Chinese Medicine in December 2018.

Acknowledgments

This work was supported by Shanghai Biotree Biotech Co. Ltd.

Author Contributions

All authors have made substantial contributions to the work reported, including conceiving the topic, designing the study, performing sample collection, acquiring, analyzing, and interpreting the data, and all authors have participated in drafting, revising, or critically reviewing the article, and have finally approved the version to be published. The submitting author has obtained authorization from all coauthors to submit the research paper, and all authors have agreed on the journal to which the article will be submitted and agree to be accountable for all aspects of the work.

Funding

The study was funded by the National Natural Science Foundation of China (82174279, 81703982). Additionally, the Shanghai Science and Technology Planning Program (21DZ2271000) contributed to the funding.

Disclosure

The authors declare that the research was conducted in the absence of any commercial or financial relationships that could be construed as a potential conflict of interest.

References

1. Rahmani A, Moradkhani A, Hafezi Ahmadi MR, Jafari HA, Abangah G, Asadollahi K. Association between serum levels of high sensitive C-reactive protein and inflammation activity in chronic gastritis patients. *Scand J Gastroenterol*. 2016;51(5):531–537. doi:10.3109/00365521.2015.1102318
2. Farthing MJ, Fairclough PD, Hegarty JE, Swarbrick ET, Dawson AM. Treatment of chronic erosive gastritis with prednisolone. *Gut*. 1981;22(9):759–762. doi:10.1136/gut.22.9.759

3. Chen SL, Mo JZ, Cao ZJ, Chen XY, Xiao SD. Effects of bile reflux on gastric mucosal lesions in patients with dyspepsia or chronic gastritis. *World J Gastroenterol*. 2005;11(18):2834–2837. doi:10.3748/wjg.v11.i18.2834
4. Watari J, Chen N, Amenta PS, et al. Helicobacter pylori associated chronic gastritis, clinical syndromes, precancerous lesions, and pathogenesis of gastric cancer development. *World J Gastroenterol*. 2014;20(18):5461–5473. doi:10.3748/wjg.v20.i18.5461
5. Noto CN, Hoft SG, Bockerstett KA, et al. IL13 Acts directly on gastric epithelial cells to promote metaplasia development during chronic gastritis. *Cell Mol Gastroenterol Hepatol*. 2022;13(2):623–642. doi:10.1016/j.jcmgh.2021.09.012
6. Zheng HR, Zhang XQ, Li LZ, et al. Multicentre prospective cohort study evaluating gastroscopy without sedation in China. *Br J Anaesth*. 2018;121 (2):508–511. doi:10.1016/j.bja.2018.04.027
7. Ye J, Cai X, Yang J, Sun X, Hu C, Xia J. Bacillus as a potential diagnostic marker for yellow tongue coating. *Sci Rep*. 2016;6(1):32496. doi:10.1038/srep32496
8. Li DY. *Dong-Yuan's Treatise on the Spleen & Stomach: A Translation of the Pi Wei Lun*. Blue Poppy Press; 2004.
9. Dong H, Guo Z, Zeng C, Zhong H, He Y, Wang RK. Quantitative analysis on tongue inspection in traditional Chinese medicine using optical coherence tomography. *J Biomed Opt*. 2008;13(1):011004. doi:10.1117/1.2870175
10. World Health Organization. *WHO international standard terminologies on traditional Chinese medicine*. World Health Organization; 2022.
11. Lundgren T, Mobilia A, Hallström H, Egelberg J. Evaluation of tongue coating indices. *Oral Dis*. 2007;13(2):177–180. doi:10.1111/j.1601-0825.2006.01261.x
12. Yoshizawa JM, Schafer CA, Schafer JJ, Farrell JJ, Paster BJ, Wong DT. Salivary biomarkers: toward future clinical and diagnostic utilities. *Clin Microbiol Rev*. 2013;26(4):781–791. doi:10.1128/CMR.00021-13
13. Hao Y, Yuan X, Yan J, et al. Metabolomic markers in tongue-coating samples from damp phlegm pattern patients of coronary heart disease and chronic renal failure. *Dis Markers*. 2019;2019:4106293. doi:10.1155/2019/4106293
14. Sun S, Wei H, Zhu R, et al. Biology of the tongue coating and its value in disease diagnosis. *Complement Med Res*. 2018;25(3):191–197. doi:10.1159/000479024
15. Chen J, Shan Y, Yan Q, et al. A metabonomics approach based on liquid chromatography-mass spectrometry: from metabolic profiling to potential biomarker. *Sci China Press*. 2009;13(10):1268–1276.
16. Li F, Zhao J, Qian P, et al. Metabolite changes in the greasy tongue coating of patients with chronic gastritis. *J Chinese Integrative Med*. 2012;10 (7):757–765. doi:10.3736/jcim20120706
17. Sun ZM, Zhao J, Qian P, et al. Metabolic markers and microecological characteristics of tongue coating in patients with chronic gastritis. *BMC Complementary Alternative Med*. 2013;13(1):227. doi:10.1186/1472-6882-13-227
18. Dixon MF, Genta RM, Yardley JH, Correa P. Classification and grading of gastritis. *Am J Surg Pathol*. 1996;20(10):1161–1181. doi:10.1097/00000478-199610000-00001
19. Piazzesi A, Afsar SY, van Echten-Deckert G. Sphingolipid metabolism in the development and progression of cancer: one cancer's help is another's hindrance. *Mol Oncol*. 2021;15(12):3256–3279. PMID: 34289244; PMCID: PMC8637577. doi:10.1002/1878-0261.13063
20. Török N, Tanaka M, Vécsei L. Searching for peripheral biomarkers in neurodegenerative diseases: the tryptophan-kynurenine metabolic pathway. *Int J Mol Sci*. 2020;21(24):9338. doi:10.3390/ijms21249338
21. Sharma G, Enriquez JS, Armijo R, Wang M, Bhattacharya P, Pudakalakatti S. Enhancing cancer diagnosis with real-time feedback: tumor metabolism through hyperpolarized 1-13C pyruvate MRSI. *Metabolites*. 2023;13(5):606. doi:10.3390/metabo13050606
22. Chen Y, Torta F, Koh HWL, et al. Metabolomics profiling in multi-ancestral individuals with type 2 diabetes in Singapore identified metabolites associated with renal function decline. *Diabetologia*. 2024;68:1–19.
23. Chen J, Sun Y, Li J, et al. In-depth metaproteomics analysis of tongue coating for gastric cancer: a multicenter diagnostic research study. *Microbiome*. 2024;12(1):6. PMID: 38191439; PMCID: PMC10773145. doi:10.1186/s40168-023-01730-8
24. Zeki ÖC, Eylem CC, Reçber T, Kır S, Nemutlu E. Integration of GC-MS and LC-MS for untargeted metabolomics profiling. *J Pharmaceut Biomed Analysis*. 2020;190:113509. doi:10.1016/j.jpba.2020.113509
25. Yifeng X, Zhang R, Morris R, et al. Metabolite characteristics in tongue coating from damp phlegm pattern in patients with gastric precancerous lesion. *Evid Based Complement Alternat Med*. 2021;2021(1):5515325. doi:10.1155/2021/5515325
26. Chang AY, Lalia AZ, Jenkins GD, Dutta T, Carter RE, Singh RJ. Combining a nontargeted and targeted metabolomics approach to identify metabolic pathways significantly altered in polycystic ovary syndrome. *Metabolism*. 2017;71:52–63. doi:10.1016/j.metabol.2017.03.002
27. Nagy K, Tiuca I-D. Importance of fatty acids in physiopathology of human body. In: *Fatty Acids*. Intech; 2017:5772/67407. doi:10.5772/67407
28. Khasawneh J, Schulz MD, Walch A, et al. Inflammation and mitochondrial fatty acid beta-oxidation link obesity to early tumor promotion. *Proc Natl Acad Sci U S A*. 2009;106(9):3354–3359. doi:10.1073/pnas.0802864106
29. Yu L, Aa J, Xu J, et al. Metabolomic phenotype of gastric cancer and precancerous stages based on gas chromatography time-of-flight mass spectrometry. *J Gastroenterol Hepatol*. 2011;26(8):1290–1297. doi:10.1111/j.1440-1746.2011.06724.x
30. Liu Y, Xu W, Qin X. Deciphering the mechanical network of chronic atrophic gastritis: a urinary time-dependent metabonomics-based network pharmacology study. *Front Physiol*. 2019;10:1004. doi:10.3389/fphys.2019.01004
31. Kim D-H, Son BK, Min K-W, et al. Chronic gastritis is associated with a decreased high-density lipid level: histological features of gastritis based on the updated Sydney system. *J Clin Med*. 2020;9(6):1856. doi:10.3390/jcm9061856
32. Tan MC, Graham DY. Gastric cancer risk stratification and surveillance after *Helicobacter pylori* eradication: 2020. *Gastrointestinal Endoscopy*. 2019;90(3):457–460. doi:10.1016/j.gie.2019.05.034
33. Ridker PM. High-sensitivity C-reactive protein, vascular imaging, and vulnerable plaque: more evidence to support trials of antiinflammatory therapy for cardiovascular risk reduction. *Circ Cardiovasc Imaging*. 2011;4(3):195–197. doi:10.1161/CIRCIMAGING.111.965053
34. Laurila A, Cole SP, Merat S, et al. High-fat, high-cholesterol diet increases the incidence of gastritis in LDL receptor-negative mice. *Arteriosclerosis Thrombosis Vasc Biol*. 2001;21(6):991–996. doi:10.1161/01.atv.21.6.991
35. Luo X, Cheng C, Tan Z, et al. Emerging roles of lipid metabolism in cancer metastasis. *Mol Cancer*. 2017;16(1):76. doi:10.1186/s12943-017-0646-3
36. Pandey S, Murphy RF, Agrawal DK. Recent advances in the immunobiology of ceramide. *Exp Mol Pathol*. 2007;82(3):298. doi:10.1016/j.yexmp.2006.07.009
37. Golden R, Gandy J, Vollmer G. A review of the endocrine activity of parabens and implications for potential risks to human health. *Crit Rev Toxicol*. 2005;35(5):435–458. doi:10.1080/10408440490920104

38. Candong L, Chengyu W. *Diagnostics of Traditional Chinese Medicine*. Beijing: China Press of Traditional Chinese Medicine; 2012:52–55.
39. Zhang XS, Zhang P, Ying Hua L, et al. Caprylic acid improves lipid metabolism, suppresses the inflammatory response and activates the ABCA1/p-JAK2/p-STAT3 signaling pathway in C57BL/6J mice and RAW264.7 cells. *Biomed Environm Sci*. 2022;35(2):95–106. ISSN 0895-3988. doi:10.3967/bes2022.014
40. Zhang X, Zhang P, Liu Y, et al. Effects of caprylic acid and eicosapentaenoic acid on lipids, inflammatory levels, and the JAK2/STAT3 pathway in ABCA1-deficient mice and ABCA1 knock-down RAW264.7 cells. *Nutrients*. 2023;15(5):1296. PMID: 36904298; PMCID: PMC10005197. doi:10.3390/nu15051296
41. Zhang XR, Luo YT, Zhu FY, et al. Novel target for treatment of colorectal cancer: metabolism and regulatory mechanisms of ferroptosis. *Shijie Huaren Xiaohua Zazhi*. 2023;31(13):528–536.
42. Conrad M, Pratt DA. The chemical basis of ferroptosis. *Nat Chem Biol*. 2019;15(12):1137–1147. doi:10.1038/s41589-019-0408-1
43. Sun Y, Chen P, Zhai B, et al. The emerging role of ferroptosis in inflammation. *Biomed Pharmacother*. 2020;127:110108. doi:10.1016/j.biopha.2020.110108
44. Zhao Z, Xiao Y, Elson P, et al. Plasma lysophosphatidylcholine levels: potential biomarkers for colorectal cancer. *J Clin Oncol*. 2007;25(19):2696–2701. PMID: 17602074. doi:10.1200/JCO.2006.08.5571
45. Afrasiabi E, Blom T, Balthasar S, Törnquist K. Antiproliferative effect of sphingosylphosphorylcholine in thyroid FRO cancer cells mediated by cell cycle arrest in the G2/M phase. *Mol Cell Endocrinol*. 2007;274(1–2):43–52. doi:10.1016/j.mce.2007.05.016
46. Müller GA, Müller TD. Biological role of the intercellular transfer of glycosylphosphatidylinositol-anchored proteins: stimulation of lipid and glycogen synthesis. *Int J Mol Sci*. 2022;23(13):7418. doi:10.3390/ijms23137418
47. Hu KW, Chen FH, Ge JF, Cao LY, Li H. Retinoid receptors in gastric cancer: expression and influence on prognosis. *Asian Pac J Cancer Prev*. 2012;13(5):1809–1817. doi:10.7314/APJCP.2012.13.5.1809
48. Hyde CA, Missailidis S. Inhibition of arachidonic acid metabolism and its implication on cell proliferation and tumour-angiogenesis. *Int Immunopharmacol*. 2009;9(6):701–715. doi:10.1016/j.intimp.2009.02.003
49. Hao Y, Zhang R, Morris R, et al. Metabolome and microbiome alterations in tongue coating of gastric precancerous lesion patients. *Expert Rev Gastroenterol Hepatol*. 2021;15(8):949–963. PMID: 33252275. doi:10.1080/17474124.2021.1850259
50. Ogretmen B, Hannun YA. Biologically active sphingolipids in cancer pathogenesis and treatment. *Nat Rev Cancer*. 2004;4(8):604–616. doi:10.1038/nrc1411
51. Jain A, Beutel O, Ebell K, Korneev S, Holthuis JC. Diverting CERT-mediated ceramide transport to mitochondria triggers Bax-dependent apoptosis. *J Cell Sci*. 2017;130(2):360–371. doi:10.1242/jcs.194191